Optics Communications 402 (2017) 311–318

Contents lists available at ScienceDirect

Optics Communications

journal homepage: www.elsevier.com/locate/optcom

Measurement error of global rainbow technique: The effect of recording parameters

Xue-cheng Wu [a], Can Li [a], Hao-yu Jiang [a], Jian-zheng Cao [a], Ling-hong Chen [a,*], Gerard Gréhan [b], Ke-fa Cen [a]

[a] State Key Lab of Clean Energy Utilization, Zhejiang University, Hangzhou 310027, China
[b] UMR 6614/CORIA, Normandie Université, CNRS, Université et INSA de Rouen, bp12 76801 Saint Etienne du Rouvray, France

ARTICLE INFO

Keywords:
Global rainbow technique
Recording parameters
Measurement error
Refractive index
Aberrations

ABSTRACT

Rainbow refractometry can measure refractive index and size of spray droplets simultaneously. Recording parameters of global rainbow imaging system, such as recording distance and scattering angle recording range, play a vital role in in-situ high accuracy measurement. In the paper, a theoretical and experimental investigation on the effect of recording parameters on measurement error of global rainbow technique was carried out for the first time. The relation of the two recording parameters, and the monochromatic aberrations in global rainbow imaging system were analyzed. In the framework of Lorenz–Mie theory and modified Nussenzveig theory with correction coefficients, measurement error curves of refractive index and size of the droplets caused by aberrations for different recording parameters were simulated. The simulated results showed that measurement error increased with RMS radius of diffuse spot; a long recording distance and a large scattering angle recording range both caused a larger diffuse spot; recording parameters were indicated to have a great effect on refractive index measurement error, but have little effect on measurement of droplet size. A sharp rise in spot radius at large recording parameters was mainly due to spherical aberration and coma. To confirm some of the conclusions, an experiment was conducted. The experimental results showed that the refractive index measurement error was as high as 1.3×10^{-3} for a recording distance of 31 cm. In the case, recording parameters are suggested to be set to as small a value as possible under the same optical elements.

1. Introduction

The parametric measurement of particles in a multiphase flow is critical to the quantitative study of fluid transport process. The accurate measurement of various parameters of spray droplets is helpful in studying the complex process of a gas–liquid two-phase flow, such as atomization cooling [1], atomizing mixing and combustion [2], absorbing and removing pollutants [3] etc. It plays an important role in the fine control of mechanical processing, improvement of combustion efficiency and reduction of pollutant emissions. Contacting methods can obtain information about spray droplets to a certain extent, but tend to cause distortion and destruction in the original flow field and no longer meet the increasingly strict requirements of spray measurement. As an advanced optical measurement method, rainbow refractometry is a type of spray measurement technique with great potential for application and development, due to its ability to measure parameters such as refractive index (*RI*), *RI* gradient [4], temperature (or composition [5]) and droplet size [6] in non-contact way.

Standard rainbow technique (SRT) for an individual droplet was proposed by Roth et al. [7]. However, high-frequency ripple structures and non-spherical droplets lead to a great measurement error of SRT. Van Beeck et al. [8] proposed the global rainbow technique (GRT) for measuring polydisperse droplets, which aims to solve these problems. By extending the exposure time and enlarging the aperture, a smooth rainbow is able to record thousands of droplets with a certain size distribution. Then the mean RI, mean diameter and size distribution of the droplets can be retrieved. Saengkaew et al. [9,10] investigated the sensitivity of GRT to the measurement of non-spherical droplets and sprays with a dependence of the *RI* on droplet size. In addition, GRT had been applied to a two-phase V-type flame for quantitatively analyzing the evolution of the mean temperature of fuel droplet [11]. Ouboukhlik et al. [12,13] successfully applied GRT to measure the mass transfer

* Corresponding author.
E-mail address: chenlh@zju.edu.cn (L. Chen).

http://dx.doi.org/10.1016/j.optcom.2017.06.018
Received 21 February 2017; Received in revised form 29 May 2017; Accepted 3 June 2017
0030-4018/

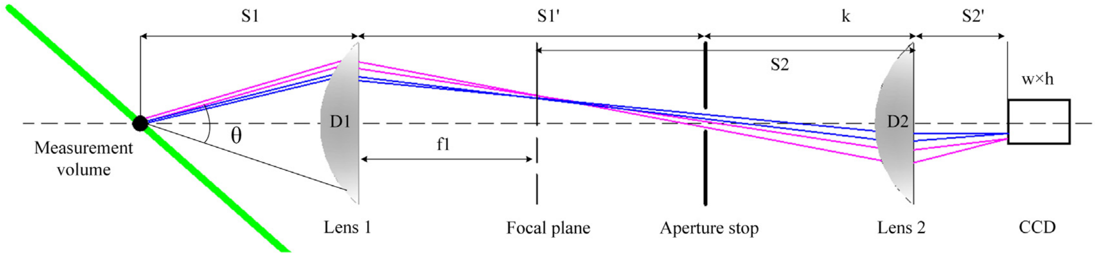

Fig. 1. Schematic diagram of the global rainbow imaging system.

coefficient and characterize the transient mass transfer evolution of a monoethanolamine solution containing 30% water in a spray tower. In recent years, GRT has been shown to be a powerful tool for diagnostics of spray in combustion and pollutant removal.

To adapt the experimental technique for use in online measuring instruments, GRT requires quantitative analysis of its measurement error. Measurement error is the combination of systematic errors and random errors, but systematic errors dominate. Systematic errors of GRT measurement are composed of errors brought about by inversion algorithm, calibration system and optical imaging system. However, mainstream researches on GRT are focused on improvements and applications of this technique [14–16]. Few investigations on measurement error of GRT, especially on measurement error from optical imaging system, have been reported in the literature. Recording distance (or working distance) is a vital parameter for GRT, and a long recording distance is widely used. The same goes for scattering angle recording range. This paper aims to study the effect of the two recording parameters of the global rainbow imaging system on measurement error.

This paper is organized as follows. Section 2 presents the theoretical relation of the two recording parameters and the monochromatic aberrations in the global rainbow imaging system. In Section 3, the effect of recording parameters on measurement error of GRT was examined and the reason for a sharp rise in spot radius at large recording parameters was analyzed. Section 4 is devoted to the presentation of an experiment designed to verify some of the results of our simulations. Section 5 provides the conclusion.

2. Analysis of the global rainbow imaging system

2.1. The relation of the two recording parameters

A global rainbow imaging system schematic diagram is displayed in Fig. 1. The system has two main components: a laser emission component and a signal receiving component. The laser emission system is composed of a laser, a mirror (or group of mirrors), a collimating system. The signal receiving system is generally composed of two convex lenses, an aperture stop and a line/area array CCD.

Lens 1 collects scattering light in the vicinity of the geometric rainbow angle of water (about 138°) in spray measurement zone, and the parallel scattering light emitted by every droplet at each scattering angle is focused by this lens and on its back focal plane. Aperture stop can effectively eliminate stray environmental light, reducing the effect of stray light through lens 2 on the CCD imaging. Adjustments to the aperture stop size and its position in the image plane of the measured droplet can also be used to select and control the measurement volume. It is more likely that the droplets in a small region have similar physical properties such as droplet size, temperature and so on. The second lens conjugates the back focal plane of the first lens on the CCD. The two spherical lenses (plano-convex) and one aperture stop, together with the CCD (width w, height h, $w > h$), form the global rainbow imaging system.

The expression for Fourier imaging system, derived from the Gaussian imaging formula, is:

$$\begin{cases} s_1 = \dfrac{D_s}{2\tan(\theta/2)}\left(D_s \le D_1\right) \\ s_1' = \dfrac{D_s f_1}{D_s - 2f_1\tan(\theta/2)} \\ s_2 = \dfrac{f_2(f_1\tan(\theta/2) + w/2)}{w/2} \\ s_2' = \dfrac{f_2(f_1\tan(\theta/2) + w/2)}{f_1\tan(\theta/2)} \end{cases} \tag{1}$$

where s_1 is recording distance from the measurement volume to lens 1, θ is scattering angle recording range, and D_s is the entrance pupil diameter of scattering light. D_1, f_1, D_2, f_2 are the diameter and focal length of the two lenses, respectively. s_2, s_1', s_2', are all intermediate quantities which show the axial position between the components. In order to meet the conditions of second-order paraxial approximation, the angle between the scattering light and the optical axis must be less than 10°.

For a fixed s_1, θ has a minimum value $\theta_{\min}$ and a maximum value $\theta_{\max}$. The $\theta_{\min}$ needs to satisfy the condition that the CCD records at least one rainbow main peak and $\theta_{\max}$ is mainly determined by the demanded image resolution. For a fixed θ, the maximum value $s_{1\max}$ and the minimum value $s_{1\min}$ are restricted by the size of lens 1 and signal intensity, respectively. Therefore, there are two mutually constrained parameters s_1 and θ which restrict the allowable range of values.

2.2. The monochromatic aberrations

Optical and imaging systems can contain multiple combinations of optical aberrations. Aberrations will always degrade rainbow image quality. The effect of these aberrations is to cause errors in the results obtained by the inversion algorithm. Therefore, the first step of our work is to recognize the different types of aberrations. It is worth noting that the global rainbow imaging system has aberrations and this phenomenon can be observed through the experimental results of scattering angle calibration by a mirror. Scattering angle calibration is the process to determine the relationship between CCD pixel and scattering angle. As illustrated in Fig. 2, a larger angle between pupil light and optical axis (i.e., the entrance pupil light close to the edge) gives a bigger speckle, which will be explained in Section 3.3. The ideal speckle size at different scattering angles remains the same in the absence of aberrations.

It is therefore necessary to explore the types of aberrations in this optical imaging system. In 1856, Seidel identified the five primary aberrations arising for monochromatic light: spherical aberration, coma, astigmatism, field curvature and distortion. These are called the five Seidel aberrations [17]. Spherical aberration occurs with all spherical optics and it is an axial aberration. The other four aberrations belong to off-axis aberrations, affecting the images increasingly toward the edge of the field but not at the center [18]. As lens 1 collects the scattering light from a small measurement volume usually viewed as an object point on the optical axis, only spherical aberration is produced in the first part